

OCEAN MICROSEISM MEASUREMENTS WITH A NEUTRAL BOUYANCY FREE-FLOATING MIDWATER SEISMOMETER

H. BRADNER, LOUIS G. DE JERPHANION* AND RICHARD LANGLOIS†

ABSTRACT

Seismometers in spherical aluminum pressure housings have been weighted to float stably at midwater depths in the ocean, and thus record water motions in a frequency band of 0.02 to 5 cps. Simultaneous records made with a midwater instrument at 1.2-km depth and a bottom instrument at 4.6-km depth showed coherence at spectral power peaks of leaky organ-pipe frequencies and additional coherence peaks at frequencies down to 0.025 cps. Twenty organ-pipe modes can be tentatively identified. The spectral power can be attributed almost entirely to microseismic motions in wave-guide modes. We conclude that the forcing functions for microseisms are broad enough so that deep ocean-bottom and midwater microseism spectral peak frequencies are characteristic of local bathymetry.

INTRODUCTION

We have modified our ocean-bottom seismometers to be neutrally buoyant at pre-determined depths in the ocean, like Swallow floats (Swallow, 1955). Such stable midwater operation is possible since the aluminum pressure cases of our instruments are less compressible than sea water. The work was initially undertaken by the first and third authors in order to study the modes of ocean wave-guide excitation that had been inferred from ocean-bottom seismic background spectra (Bradner and Dodds, 1964). The second author joined the work for his master's degree thesis project. Additional motivation for the work arose from our belief that water motion around ocean-bottom instruments may mask seismic background spectra at frequencies lower than the microseism peak. A free-floating neutrally buoyant instrument will move almost exactly as the surrounding water and hence will not produce signals due to steady water flow. The correspondence is not quite exact because the compressibility of the instrument is not the same as water. The center of mass of the instrument is displaced from the geometrical center, and the seismometer has a small spring-supported mass which moves with respect to the center of mass of the instrument.

OCEAN WAVE-GUIDE MODES

The general equation for the displacement potential of small amplitude elastic wave motion in a homogeneous fluid is the simple wave equation

$$\frac{\partial^2 \psi}{\partial t^2} = c^2 \frac{\partial^2 \psi}{\partial x^2}.$$

If we consider a source to be an antinode of pressure oscillations on a rigid bottom interface, and consider the air above the top interface to be massless, we can write the

* Present address: Intertechnique, 78 Plaisir, Paris France.

† Present address: Department of Chemistry, Columbia University Graduate School, New York, New York 10021.

solution of the wave equation as a plane wave

$$\psi = 2A \sin (2\pi ft) \sin (2\pi x/\lambda)$$

with wavelength $\lambda = 4H/(2n + 1)$, where x is the depth of observation and H is the water depth. This model would predict “organ-pipe” resonant modes in the ocean wave guide. More realistic models with distant sources and semirigid layered bottoms lead to a somewhat similar mode structure, although the frequencies are not always exact multiples of the fundamental, and they may show different excitation amplitudes. Also, there is not an amplitude node at the ocean bottom for most modes. (See for example Chapter 4 of Ewing, Jardetzky and Press, 1957.)

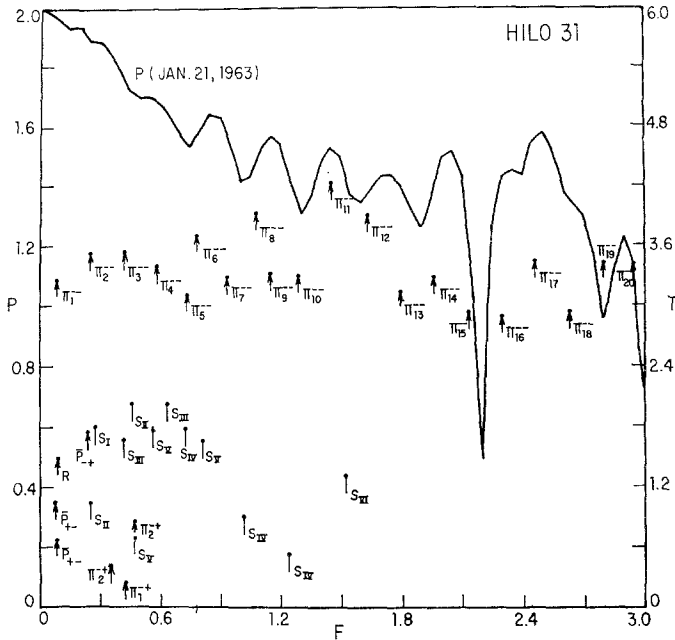


FIG. 1. (Reproduced from Abramovici, 1968.) Power density spectrum P on ocean bottom, January 21 1963 (Bradner and Dodds, 1964). Location: $22^{\circ} 28'N, 158^{\circ} 00'W$. The isolated points show peaks of the transfer function T for Hilo 31 with the attenuation factor $A = e^{-(0.002F_i^2/a)}$. The scales for P (left) and T (right) are logarithmic.

Abramovici (1968) computed the modes for a layered bottom. He shows that these modes reproduced in Figure 1 are in good agreement with measured ocean-bottom power spectra (Bradner and Dodds, 1964). In all cases, the water surface is a displacement antinode. Hence the ratio of midwater power to bottom power in vertical organ-pipe modes can be written readily as:

$$\frac{\cos^2 2\pi fx/c}{\cos^2 2\pi fH/c}$$

where f is the frequency of the leaky organ-pipe mode, x is the depth of the midwater observation, H is the water depth and c is the velocity of compressional waves in water. The power ratio for modes other than vertical organ pipe generally cannot be expressed in this simple form.

INSTRUMENTS

The basic instruments were our ocean-bottom seismometers, consisting of California Institute of Technology/United Electroynamics 1-cps lunar velocity transducer seismometers in orthogonal triaxial arrangement with tape recorders in 65-cm diameter aluminum pressure cases (Bradner and Dodds, 1964). For midwater use, the anchor was replaced by a counterweight of the proper net weight to make the instrument float at a predetermined depth in ocean water. The counterweight was attached in a manner similar to the anchor of the ocean-bottom instrument, and was released at a predetermined time by electrolytic solution of a magnesium pin. A supplementary weight of approximately 10 kg was employed to sink the instrument rapidly to near the desired operating depth, where this weight was released by the bursting of a calibrated diaphragm. A pressure transducer was mounted on the instrument to record its depth on a

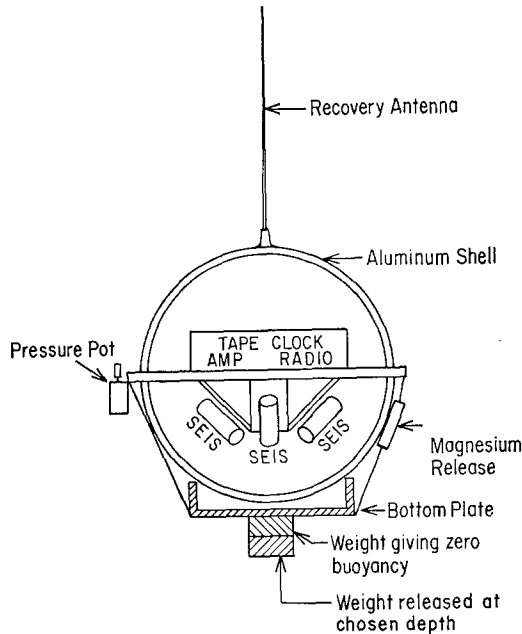


FIG. 2. Schematic view of midwater seismometer. Three-component triaxial seismometer is contained in aluminum pressure housing, along with amplifiers, crystal clock, tape recorder and radio recovery beacon transmitter.

Rustrack recorder or on one frequency-modulated track of the magnetic tape recorder. A three-component instrument is shown schematically in Figure 2.

MOTION OF A NEUTRALLY BUOYANT INSTRUMENT

When the instrument is near its equilibrium depth in still water, its free oscillatory motion is characterized by the float compressibility and the Väisälä frequency. [The Väisälä frequency is a measure of the adiabatic oscillation stability of a small mass of fluid (for example see Eckart, 1960 and Hill, 1962). The float frequency is slightly higher than the Väisälä frequency.] The accelerations associated with this damped motion below the thermocline are negligible within the 0.02–5 cps passband of our instruments. If the center of mass of the instrument were at its center of buoyancy, and if no interior parts were flexibly mounted, then, after reaching equilibrium depth, the instrument would follow all nonrotational or shear-free motions of the water in our passband. Since

the center of mass hangs directly below the center of buoyancy and the seismometer mass is negligibly small, we can say with adequate validity that the instrument follows the vertical water motion. Water motion due to compressional waves can be considered shear-free in our observations, since the wavelength is very much larger than the dimensions of the instrument.

Horizontal water motion can produce seismometer signals by rocking the instrument with moderately low damping at its natural rocking frequency. This frequency is a function of the moment of inertia and the location of the center of mass, and in our instruments produced a discernible spurious power peak at 0.39 ± 0.01 cps in water tank tests. The rocking oscillations were less violent in the ocean experiments, and were unobservable in an experiment at 1210-m depth.

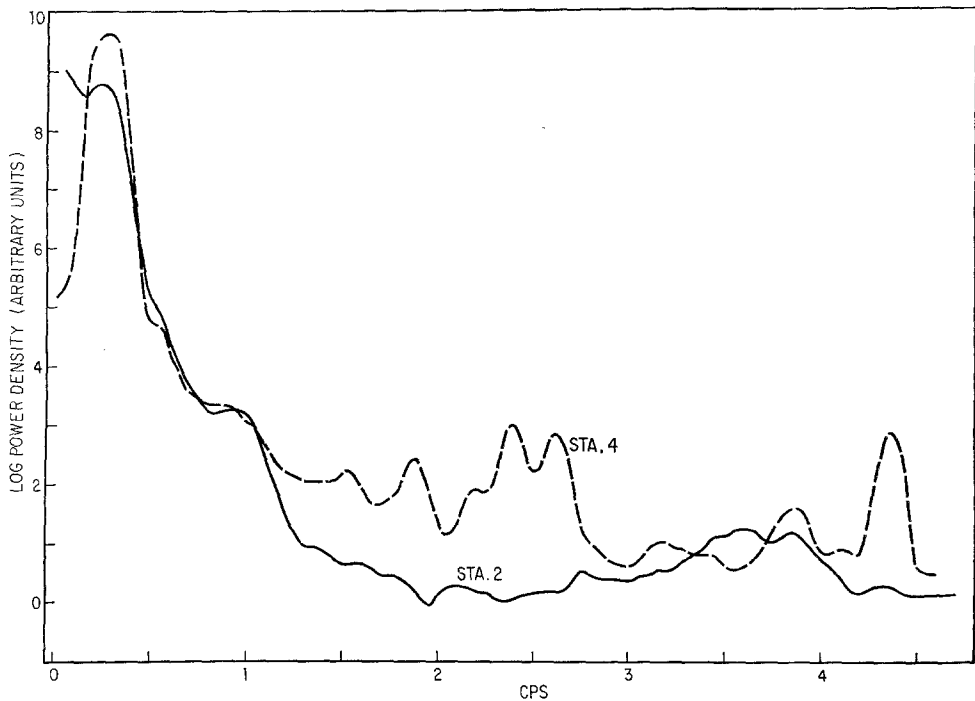


FIG. 3. Comparison of vertical power spectra for midwater seismometer, stations 2 and 4.

The release of the counterweight is accomplished through the electrolytic etching of a magnesium pin. This produces an effective change in instrument buoyancy of 0.3 gm in 4 hr. Since a 1-gm change in buoyancy causes a 3-m change in equilibrium depth the dissolving magnesium produces a small average vertical velocity of 6.25×10^{-3} cm sec⁻¹. Accelerations associated with this average velocity should be negligibly small.

We believe therefore that the midwater instrument gives a valid indication of water motion in the frequency range from 0.02 to 5 cps. The main motion is expected to be due to compressional waves, although the ocean is a stratified fluid with unknown flows that can also arise from internal waves and driven motions. The frequencies of internal waves are expected to lie outside our passband but we cannot exclude *a priori* the possibility of spurious signals from unknown driving forces.

EXPERIMENTAL RESULTS

Near-Shore Observations. Station 2 was run in a water depth of 1500 ± 50 m over broken bottom at a location 24 km southwest of San Diego. Throughout a 4-hr period

the instrument stayed at a constant depth of 430 m within the resolution of the depth recorder (± 40 m).

Station 4 was run in the same water depth, within 10 km of station 2. The instrument depth was 800 ± 40 m. The two runs were separated in time by 7 months. Original analog magnetic tape records were digitized on an Adage computer, using time markers that had been recorded on the tape during the seismic measurements. The digitized records from the three-component triaxial seismometers were rotated during spectral analysis on a CDC digital computer to yield vertical and horizontal spectral power densities and coherences.

Figure 3 shows the vertical spectra from the two observations. The apparent peak in power density at 0.34 cps is due to the natural rocking period of the instrument, and prevents a comparison between the spectra between about 0.3 and 0.5 cps. The spec-

TABLE 1
PEAKS IN VERTICAL SPECTRUM, STATIONS 2 AND 4

Frequency (cps)	
Station 2	Station 4
0.25	0.27
0.55	0.55
0.95	(0.9)
(1.35)	
(1.6)	1.55
(1.75)	
	1.9
2.1	2.2
	2.4
	2.6
2.75	
	3.2
3.65	
3.85	3.85
	(4.1)
4.35	4.35

tra outside of this band show several common power peaks (see Table 1), implying that the microseism background may have a peaked structure whose frequencies are characteristic of the bathymetry, and whose amplitudes are indicative of a nonwhite forcing function. The frequencies of leaky organ-pipe modes have not been calculated for this geographic region.

Deep-Water Observations. The midwater seismic measurement of station 5 was a 16-hr record in water of 4.6-km depth over a uniform bottom at a location 78 km north of Oahu, Hawaii (Figure 4). A south-southwest moving swell ran 2 to 4 m high during the experiment. The three-component triaxial seismometer floated at a depth of 1210 ± 40 m. A simultaneous record was made on the uniform flat bottom with a similar instrument. The instruments were equipped with low-noise Texas Instrument Company parametric amplifiers, and the 1-cps seismometers were low-pass filtered at 0.1 cps.

Qualitative comparison can be made between the spectral structure observed in this

experiment, at $22^{\circ}, 25'N, 158^{\circ}, 08'W$ (location by sextant) and the spectral structure observed 4 years earlier with a bottom seismometer at a nearby location, $22^{\circ}, 28'N, 158^{\circ}, 00'W$. The spectrum from the earlier observation is reproduced here as Figure 5. The upper frequencies in the spectrum from the present experiment are suppressed by the low-pass filter, so that the spectrum is not unambiguously discernible above background for frequencies higher than 1 cps. However, the midwater versus bottom coherence peaks discussed below (Figure 10) indicate that the mode structure continues out to at least 4 cps and has similar peak frequencies during both observations. Four

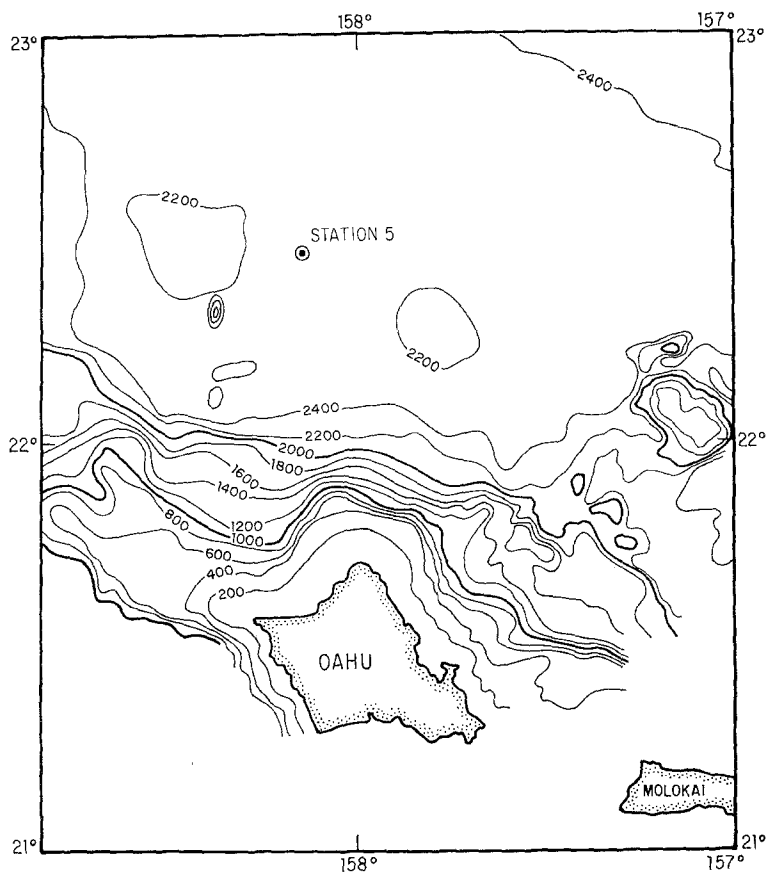


FIG. 4. Bathymetry in vicinity of station 5.

sections of data were analyzed: the first record started 6 hr after the bottom instrument was launched. Additional 2-hr length records were analyzed from 0 to 4 cps from midwater and bottom instruments, beginning at 10 hr, 14 hr and 18 hr after launching the bottom instrument. Both instruments showed small changes in spectral power distribution during the recording time, although the peak frequencies did not change.

Figure 6 shows the X , Y and Z spectra from the midwater instrument out to 4 cps during the last recording interval. The spectra have been displaced vertically in the figure for clarity: The power density between 2 and 4 cps is very nearly the same for each component. Figure 7 is a similar display for the bottom instrument. The spectral shapes from the two instruments are strikingly similar and show apparent resonance peaks in vertical power.

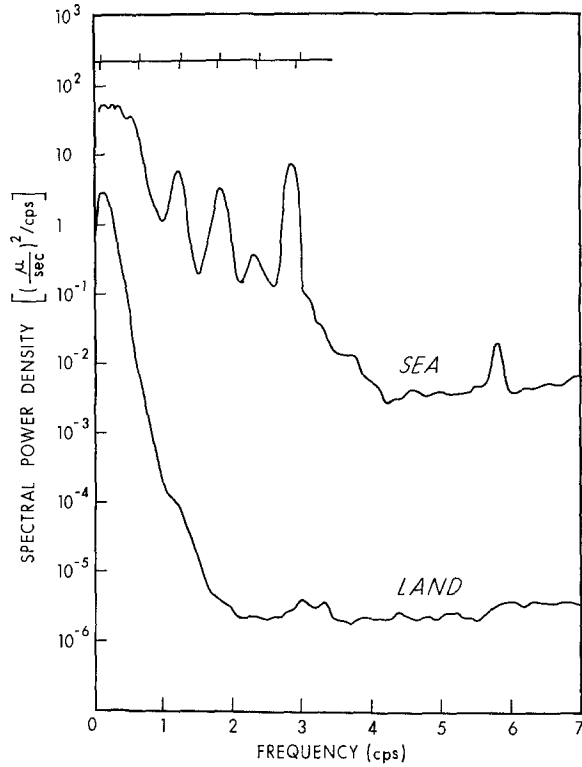


FIG. 5. (Reproduced from Bradner and Dodds, 1964.) Seismic background spectra on land and ocean bottom, February 8 1963, Hawaii. The land instrument was a vertical seismometer. The ocean-bottom instrument contained three-component equiaxial seismometers. Only one component is displayed. The other two components were similar. The scales at the top of the figure show the frequencies of organ-pipe modes in the water.

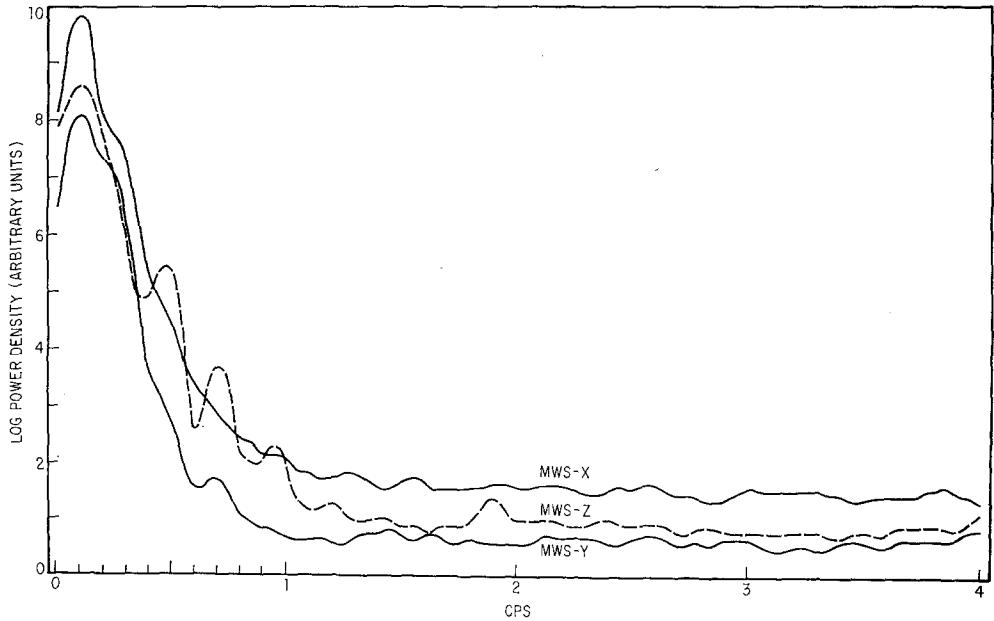


FIG. 6. Horizontal and vertical power spectra to 4 cps. Midwater seismometer, Hawaii, station 5. The plots have been displaced vertically by different amounts for clarity. Actual X:Y:Z power densities averaged over the range 2 to 4 cps are in the ratio 1:1.20:1.10.

Figures 8 and 9 show higher resolution spectra from the two instruments below $\frac{1}{2}$ cps during the last recording interval. The pronounced peaks at 0.05, 0.1 and 0.2 cps in the midwater seismometer (MWS) record are not clearly evident in the bottom record.

In all instances the time series for station 5 consisted of 7200 terms, beginning at 18 hr. Thus the 4-cps records and the $\frac{1}{2}$ -cps records were analyzed during overlapping but

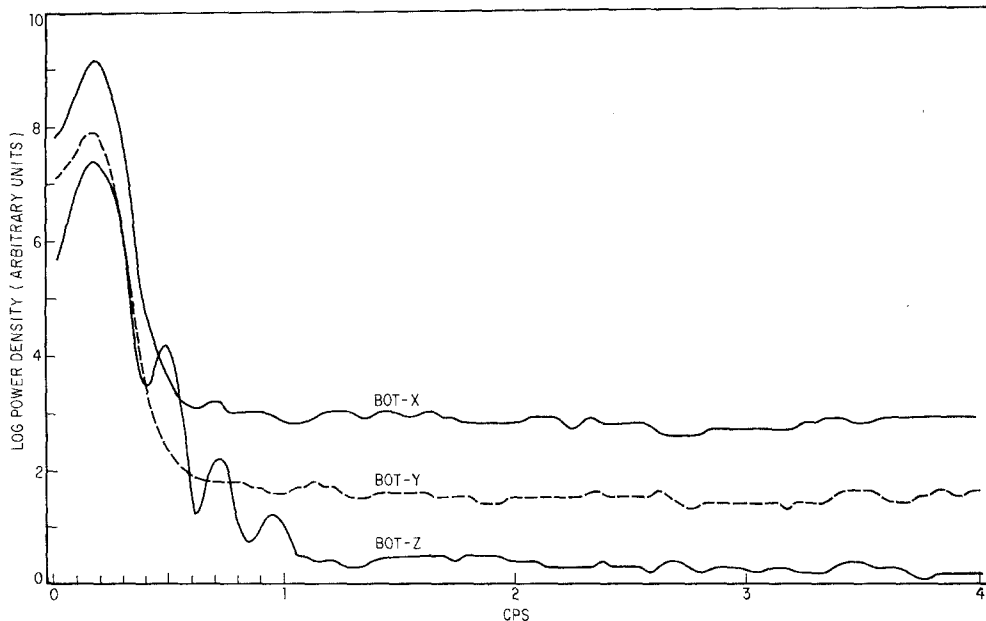


FIG. 7. Horizontal and vertical power spectra to 4 cps, bottom seismometer, Hawaii, station 5. The plots have been displaced vertically by different amounts for clarity. Actual X:Y:Z power densities averaged over the range 2 to 4 cps are in the ratio 1:1.48:1.10.

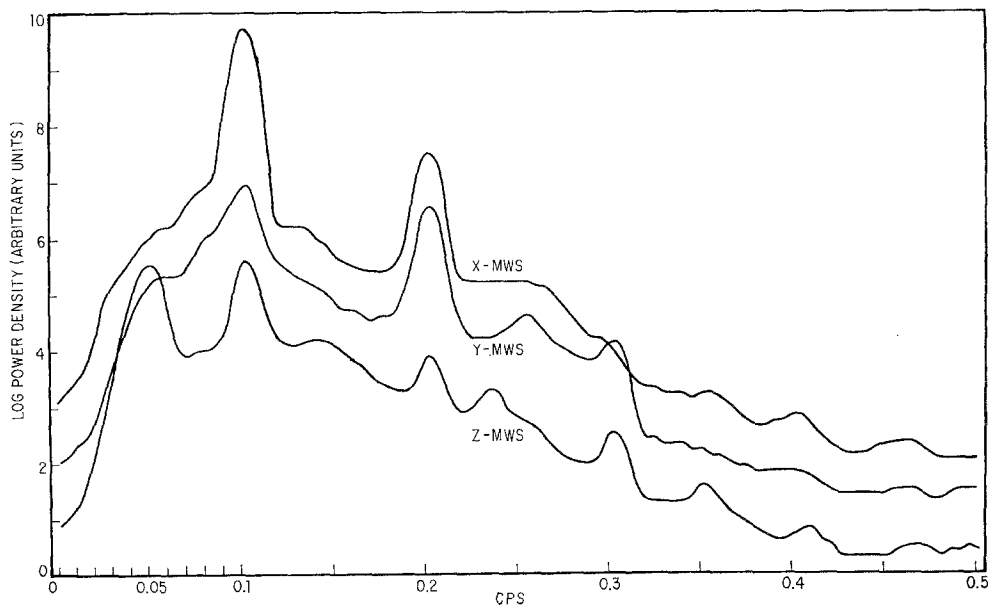


FIG. 8. Horizontal and vertical power spectra to $\frac{1}{2}$ cps, midwater seismometer, Hawaii, station 5. The plots have been displaced vertically by different amounts for clarity.

not identical times. Information on the statistical parameters for the power spectra at all stations is given in Table 2.

A large persistent power difference between *X* and *Y* in the 0.1-cps peak during the analyses at $\frac{1}{2}$ cps implies that the midwater seismometer turned through about 45° during the 16-hr period.

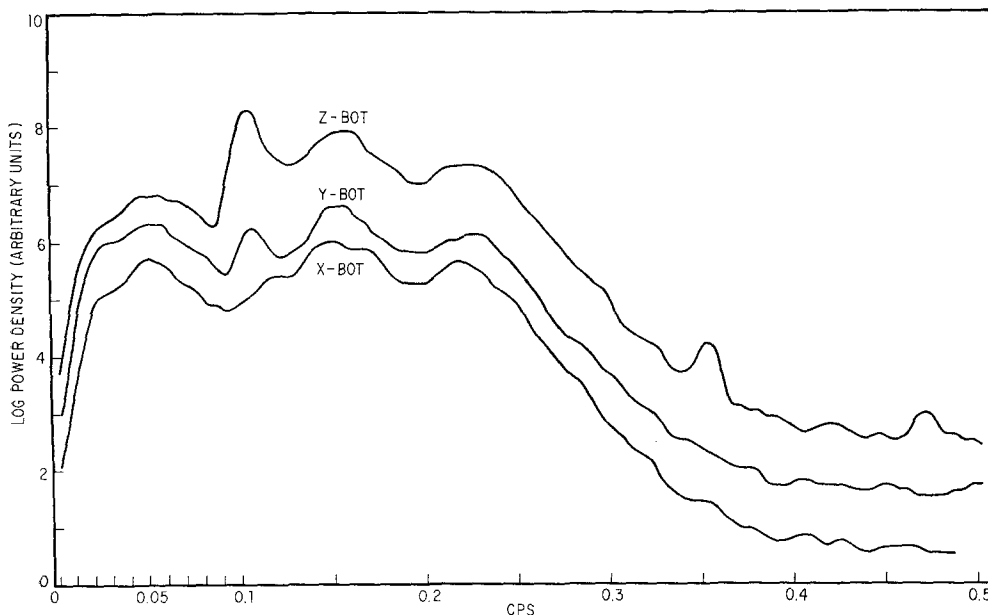


FIG. 9. Horizontal and vertical power spectra to $\frac{1}{2}$ cps. Bottom seismometer, Hawaii, station 5. The plots have been displaced vertically by different amounts for clarity.

TABLE 2
TIME SERIES USED IN CALCULATING POWER SPECTRA IN THIS PAPER

Figure	Station	Series Length (min)	No. of Terms	Samples/Sec	No. of Lags	No. of Degrees of Freedom
3	2	$3\frac{3}{4}$	4107	18.2	180	46
	4	6	6479	18.2	180	72
5	—	8	8648	18	200	90
6	5	15	7200	8	100	144
7	5	15	7200	8	100	144
8	5	120	7200	1	100	144
9	5	120	7200	1	100	144
10	5	15	7200	8	100	144

Sections of the original analog records were examined on a Panoramic RTA-5 spectrum analyzer to determine that the observed spectral shape and peak structure were valid and were not artifacts produced by the digital analysis.

Figure 10 shows the vertical component spectra from the two instruments and their coherence. In this figure the spectra have not been displaced vertically; they indicate true relative power in the midwater and bottom vertical motions.

High resolution calculations of relative amplitude, coherence and phase between *X*, *Y* and *Z* components of the MWS record show that the 0.05-cps peak is a vertically moving compressional wave, while the 0.1-cps peak comes from horizontal motion.

The power density in the 0.05-cps peak of the MWS is two orders of magnitude greater than the bottom, while the power density in the 0.1-cps peak is one order of magnitude greater than the bottom. Another small peak in the MWS record at 0.35 cps shows greater than 95 per cent confidence coherence with the bottom record. The 0.05-, 0.1- and 0.35-cps coherent peaks represent high Q wave-guide excitation modes which we feel are characteristic of the physical environment rather than peaks in a forcing function.

The weak signal at frequencies above 1 cps makes coherence low. However if we tabulate all well-defined vertical power coherent peaks regardless of size we find remarkably close agreement with the frequencies of leaky organ-pipe modes calculated by Abramovici (1968). (See Table 3.) By looking at only the vertical coherence we will

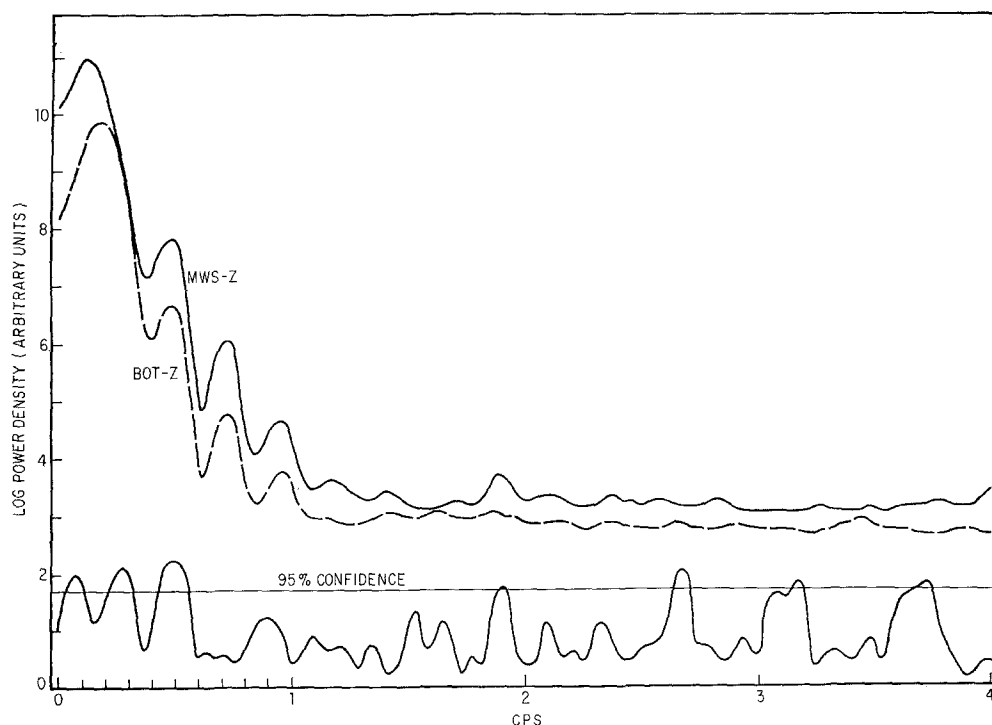


FIG. 10. Coherence between midwater and bottom seismometer power spectra, Hawaii, station 5. Midwater and bottom spectral powers can be directly compared in the figure.

overlook other possible modes, and the agreement with organ-pipe modes may be illusory.

High-resolution analysis showed that there is no power peak at 0.09 cps corresponding to the fundamental organ-pipe mode (Figure 8). The high coherence peak at 0.10 cps was shown by amplitude and phase comparison to be almost entirely horizontal X motion. The 0.05-cps peak, which may have significant coherence with the bottom record, is almost entirely Z motion. The incoherent peak at 0.20 cps is horizontal with equal power in X and Y . Vertical power coherence is high at 0.35 and at 0.45 cps although no power peak shows above the background at 0.45 cps.

By calculating spectral coherences and phases with shifted start times on the MWS time series, we found indication that the bottom seismometer lagged approximately 3 sec behind the MWS, thus supporting the idea that we are observing modes whose

energy flows downward past the floating instrument toward the bottom. We were also able to determine that the high frequency spatial coherence diminished rapidly for shifts greater than about 8 sec, thus indicating that the wave guide Q plus the forcing function for ≈ 4 -cps waves has a time coherence of about 30 cycles. Similar measurements on the 0.10-cps peak show that its time coherence is greater than 40 cycles (400 sec), while the peak at 0.35 cps has a time coherence between 72 and 144 cycles (200 to 400 sec).

TABLE 3
FREQUENCIES OF OBSERVED POWER PEAKS COMPARED WITH FREQUENCIES OF
ABRAMOVICI'S* CALCULATED MODES: STATION 5

Mode	Frequency (cps)	
	Abramovici*	Observed†
1	0.09	0.08‡
2	0.25	0.26
3	0.42	0.45
4	0.58	0.64
5	0.73	0.72
6	0.78	
7	0.93	0.88
8	1.08	1.08
9	1.14	1.20
10	1.28	1.32
11	1.45	1.52
12	1.62	1.64
13	1.78	1.76
14	1.95	1.90
15	2.12	2.08
16	2.29	2.20
17	2.45	2.32
		2.52
18	2.62	2.64
19	2.78	2.76
20	2.93	2.92

* Frequencies were read from Abramovici's (1968) plots and are uncertain to about ± 0.01 cps below mode 10, and about ± 0.02 cps in the higher modes.

† Observed frequencies were determined by peaks in coherence between MWS and BOT instruments. Peak position accurate to ± 0.02 cps (see Figure 10).

‡ Higher resolution analysis shows that the high coherence peak occurs at 0.10 cps, and there may be also statistically significant peaks around 0.05 and 0.36 cps.

We are unable to make a direct test of organ-pipe modes by comparing midwater power with bottom power at the coherent peaks, since the signal/noise ratio was severely reduced by the low-pass filter. We attempted to make a qualitative test by arguing that coherence will be reduced wherever the term $\cos^2 2\pi fx/c$ or $\cos^2 2\pi fH/c$ is small. The agreement appeared qualitatively valid above 2 cps but was not conclusive.

On the basis of all our experimental data we conclude that the seismic background at frequencies up to at least 4 cps may be carried in well-defined wave-guide modes where the bottom is uniform over a distance of several wavelengths. Leaky organ-pipe modes

are probable. Abramovici (1968) has obtained a good theoretical fit to our 1963 data by assuming a white forcing function. However, our additional data indicate that an uneven and time-varying forcing function is operative. Alternatively, we might say that the generating zone of microseisms according to the model of Haubrich (1963) can be characterized by wave-guide modes, especially leaky organ-pipe modes, with a nonwhite forcing function. This is in agreement with earlier ocean-bottom three-component seismic records which indicated organ-pipe modes near land masses, converting to Rayleigh waves at greater distance from shore (Bradner, Dodds and Foulks, 1965).

ACKNOWLEDGMENTS

We wish to thank the many members of IGPP for their counsel and help.

This research was supported by the Advanced Research Projects Agency of the Department of Defense and was monitored by the Air Force Office of Scientific Research under Contract AF 49(638)-1388.

REFERENCES

- Abramovici, F. (1968). Diagnostic diagrams and transfer functions for Oceanic wave-guides, *Bull. Seism. Soc. Am.*, **58**, 427-456.
- Bradner, H. and J. G. Dodds (1964). Comparative seismic noise on the ocean bottom and on land, *J. Geophys. Res.* **69**, 4339.
- Bradner, H., J. G. Dodds and R. E. Foulks (1965). Investigation of micro-seism sources with ocean bottom seismometers, *Geophysics* **30**, 511-526.
- Eckart, *Hydrodynamics of Oceans and Atmospheres*, Pergamon, London, 1960.
- Ewing, Jardetzky and Press. *Elastic Waves in Layered Media*, McGraw-Hill, 1957.
- Haubrich, R. A., W. H. Munk, and F. E. Snodgrass (1963). Comparative spectra of microseisms and swell, *Bull. Seism. Soc. Am.* **53**, 27-37.
- Swallow, J. C. (1955). A Neutral-buoyancy float for measuring deep currents, *Deep Sea Res.* **3**, 74-81.

INSTITUTE OF GEOPHYSICS AND PLANETARY PHYSICS
UNIVERSITY OF CALIFORNIA, SAN DIEGO
P.O. Box 109
LA JOLLA, CALIFORNIA 92037

Manuscript received January 27 1970.